Graphene growth by molecular beam epitaxy on the carbon face of SiC

Article *in* Applied Physics Letters · December 2010

DOI: 10.1063/1.3526720 · Source: OAI

9 authors, including:

Sylvie Godey
Autonomous University of Barcelona
53 PUBLICATIONS **949** CITATIONS
SEE PROFILE

F.J. Ferrer
Universidad de Sevilla
66 PUBLICATIONS **892** CITATIONS
SEE PROFILE

J. Avila
SOLEIL synchrotron
185 PUBLICATIONS **6,770** CITATIONS
SEE PROFILE

APPLIED PHYSICS LETTERS **97**, 241907 (2010)

Graphene growth by molecular beam epitaxy on the carbon-face of SiC

E. Moreau,[1,a)] S. Godey,[1] F. J. Ferrer,[1] D. Vignaud,[1] X. Wallart,[1] J. Avila,[2] M. C. Asensio,[2]
F. Bournel,[3] and J.-J. Gallet[3]
[1]*IEMN, UMR CNRS 8520, Avenue Poincare, P.O. Box 60069, 59652 Villeneuve d'Ascq Cedex, France*
[2]*Synchrotron SOLEIL, L'Orme des Merisiers, Saint Aubin-BP 48, 91192 Gif sur Yvette Cedex, France*
[3]*LCPM, Université Pierre et Marie Curie, UMR CNRS 7614, 75231 Paris Cedex, France*

(Received 19 July 2010; accepted 22 November 2010; published online 13 December 2010)

Graphene layers have been grown by molecular beam epitaxy (MBE) on the $(000\bar{1})$ C-face of SiC and have been characterized by atomic force microscopy, low energy electron diffraction (LEED), and UV photoelectron spectroscopy. Contrary to the graphitization process, the step-terrace structure of SiC is fully preserved during the MBE growth. LEED patterns show multiple orientation domains which are characteristic of graphene on SiC $(000\bar{1})$, indicating non-Bernal rotated graphene planes. Well-defined Dirac cones, typical of single-layer graphene, have been observed in the valence band for few graphene layers by synchrotron spectroscopy, confirming the electronic decoupling of graphene layers. © *2010 American Institute of Physics*. [doi:10.1063/1.3526720]

Graphene is well known for its remarkable electronic properties as studied in the recent years. From the different proven methods of fabrication, graphene has been mainly elaborated by high temperature annealing (graphitization) of silicon carbide,[1,2] by exfoliation of graphite,[3] and by chemical vapor deposition (CVD).[4,5] Both exfoliation and CVD impose to transfer the graphene layers on other insulating substrates, while graphene on SiC can be directly used for electronic transport studies and related applications. The graphitization consists in simultaneous Si sublimation and reorganization of the remaining C. SiC is a polar material and it is now well established that the graphene properties strongly depend on the considered SiC-face.[1,2] On the (0001) Si-face, a C-rich interface layer, which leads to the $(6\sqrt{3}\times 6\sqrt{3})R30°$ reconstruction, induces a strong interaction of the graphene with the substrate. The graphene lattice is rotated by 30° compared to the SiC one, with the graphitelike Bernal stacking of graphene planes. On the $(000\bar{1})$ C-face, there is no such interface layer and the coupling between the graphene layers and the SiC is so weak that uncoupled rotated graphene domains are obtained.[6–8] The monolayer graphene behavior is thus preserved even for thick layers ($\approx$10 layers), especially the linear dispersion of the band structure around the K-point.[6] One limitation of the graphitization on the C-face of SiC comes from its high growth rate,[9] which makes obtaining thin homogeneous graphene layers a difficult process.

Even if molecular beam epitaxy (MBE) is a well known process for semiconductor growth, it has only recently been used to grow graphene on SiC,[10,11] silicon,[12] and sapphire substrates.[13] The present study focuses on the MBE growth of graphene on SiC $(000\bar{1})$, showing the interest of using this alternative method on SiC carbon-face, without the degradation of the surface topography[10] induced by the graphitization process.

6H and 4H SiC $(000\bar{1})$ n-type commercial wafers were polished by NovaSiC to remove scratches and most other surface defects. A thin tungsten film was deposited onto the rear face to allow ultrahigh vacuum (UHV) noncontact radiation heating and the wafers were then diced into 4×4 mm^2 substrates. Growth was achieved in an UHV MBE chamber. The reported temperatures were measured using an optical pyrometer. Surface preparation, after a degassing step in the 800–900 °C temperature range, consisted in a long surface smoothening under Si flux exposure at 1050–1100 °C.[14] To avoid the occurrence of graphitization, the sample temperature was then lowered to 1030–1050 °C before the MBE graphene growth, for which carbon was sublimated from a high temperature heated graphite filament cell (MBE-Komponenten). The carbon flux has been estimated to be roughly $\approx 7\times 10^{12}$ atoms/(cm^2 s).

The surface crystallographic structure was investigated in another UHV chamber using low energy electron diffraction (LEED). Its topographic characterization was achieved by atomic force microscopy (AFM) in tapping mode. The chemical structure was studied by x-ray photoemission spectroscopy (XPS) carried out using Al Kα ($h\nu$=1486.6 eV) radiation from a monochromatic x-ray source and a hemispherical energy analyzer. Angle resolved XPS was used to calculate the graphene thickness.[10] Valence band dispersion was studied by angle resolved UV photoelectron spectroscopy (ARUPS) at the ANTARES beam line of the SOLEIL synchrotron.

Surface topography was controlled by AFM analysis before and after growth. Comparison between a substrate after surface preparation [Fig. 1(a)] and 60 min growth at

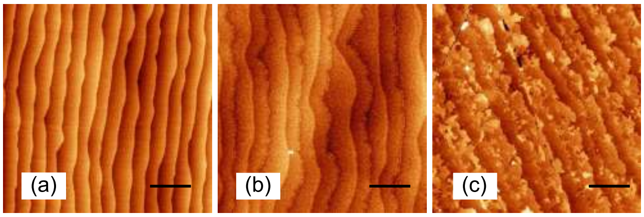

FIG. 1. (Color online) AFM topographic pictures of 6H-SiC $(000\bar{1})$ after initial surface preparation (a), after MBE growth (60 min at 1040 °C) (b), and after graphitization (10 min at 1140 °C) (c). Vertical scale: 2 nm; scale bar=2 μm.

[a)] Electronic mail: eleonore.moreau@ed.univ-lille1.fr.

0003-6951/2010/97(24)/241907/3/$30.00

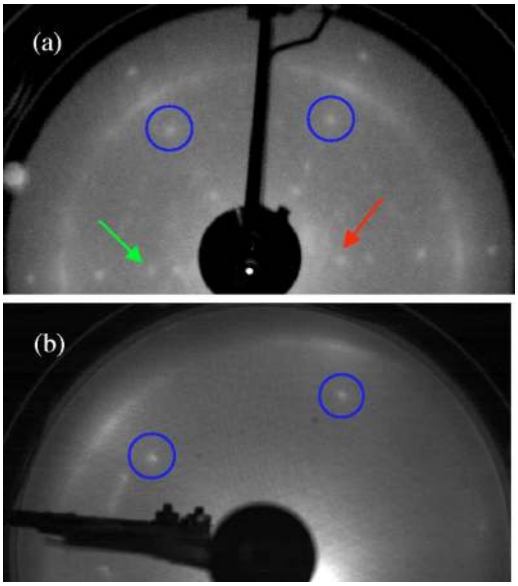

FIG. 2. (Color online) LEED images of MBE graphene grown for 25 min at 1040 °C (a) and 40 min of MBE growth (b). Left and right arrows indicate (2×2) and (3×3) reconstruction spots, respectively, while the SiC (1×1) spots are shown inside circles.

1040 °C [Fig. 1(b)] shows a step-terrace structure, almost unaffected by the MBE growth. The terrace surface rms roughness is higher on the graphene surface (roughness =0.14 nm) than after smoothening (roughness=0.05 nm). The AFM image of a graphene sample obtained by 10 min graphitization at 1140 °C, a temperature/duration combination slightly above the graphitization threshold, is also shown for comparison in Fig. 1(c). Although the step and terrace structure is still visible, the onset of graphitization and the resulting surface modification are obvious in Fig. 1(c). Since such typical features are clearly not observed after MBE growth [Fig. 1(b)], it is concluded that the graphene characteristics observed in the following result from MBE graphene without any significant contribution from graphitization.

The MBE graphene thickness has been studied as a function of the growth time by XPS. Only two components are identified on the experimental curves (not shown), respectively, located at 282.6 and 284.6 eV and corresponding to C–Si and C–C bonding. These spectra are fully consistent with previous XPS analysis of graphene obtained by graphitization.[6,15,16] For example, a film thickness of 1.8±0.5 ML is found after 25 min of MBE growth at 1040 °C. The graphene component intensity increases while the bulk peak decreases with longer growth time, as expected. An average graphene growth rate of 0.05 ML/min is deduced in good agreement with a carbon flux of $\approx 7 \times 10^{12}$ atoms/$(\mathrm{cm}^2\ \mathrm{s})$.

Crystallography of surfaces has been studied versus the growth time starting from the (1×1) SiC prepared surface, in real time by reflected high energy electron diffraction (RHEED), and after growth by LEED. After 25 min at 1040 °C, the LEED pattern simultaneously displays the C-rich (2×2) and (3×3) surface reconstructions together with the graphene-related arcs oriented 0° with respect to the substrate [Fig. 2(a)]. For thicker graphene layers, both the (2×2) and (3×3) surface reconstructions disappear: the graphene arcs and the (1×1) SiC spots are then only observed [see Fig. 2(b)]. For even thicker layers, the SiC (1×1) spots finally vanish and the graphene contribution only remains (not shown here). It must be pointed out that the successive surface reconstructions observed during MBE growth of graphene are identical to the ones observed during the graphitization process.[1,6,17] The graphene pattern is made of arcs, which means that rotated domains or stacking of rotated graphene planes exist with respect to the SiC substrate. This is a typical feature of graphene grown on the C-face of SiC.[6,18] It directly results from the weak coupling between graphene and the SiC substrate,[7,8] but also between successive graphene planes.[7] Although these observations may look similar to the study of Al-Temimy *et al.*,[11] it is worth mentioning that their growth work started on the heated-induced (3×3) C-rich surface. This (3×3) reconstruction is a mandatory pathway toward graphene growth during graphitization.[1,8] So, a contribution of the graphitization to the observations on SiC (000$\bar{1}$) reported in Ref. 11 cannot be excluded. This restriction does not apply to the present study, where MBE growth has been started directly on the (1×1) SiC (000$\bar{1}$). Some RHEED pictures taken along the [1-210] and [1-100] azimuths are presented in Fig. 3. They clearly show that different orientations of MBE graphene are observed from the beginning of the growth, at least distributed a few degrees around the [1-210] and [1-100] directions. This observation suggests that growth immediately starts along different orientations in separated domains, as already observed for graphene obtained by graphitization.[6,8,19] For longer growth time (not shown), graphene along the SiC [1-210] direction is predominant which is confirmed by the LEED picture [Fig. 2(a)].

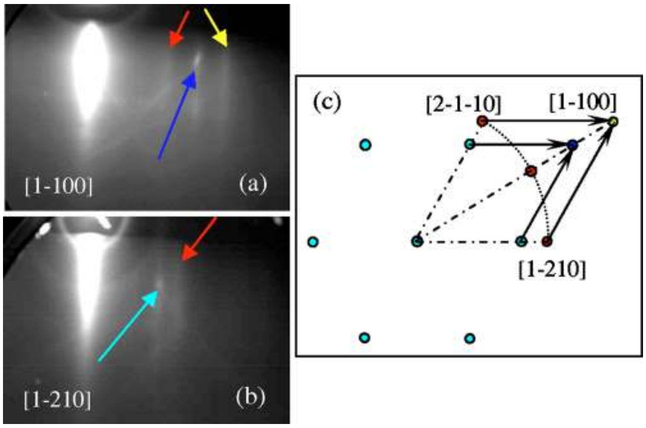

FIG. 3. (Color online) Graphene and SiC RHEED patterns after MBE growth (1050 °C for 10 min) along the [1-100] (a) and [1-210] (b) directions. Schematic of the graphene on SiC reciprocal lattice (c).

The remarkable properties of MBE graphene on SiC (000$\bar{1}$) have been confirmed by studying the valence band structure through ARUPS experiments along the Γ-K-M axis at a photon energy of 110 eV and a temperature of 100 K. For 1.8 ML growth, the σ-band and π-band are clearly observed [see Fig. 4(a)] and are well in agreement with previous results for similar thickness of graphene obtained by graphitization.[6,20] Enlargement in Fig. 4 shows the Dirac cone (b) with continuous linear dispersion up to the Fermi level. A thicker MBE graphene film (3 ML) presents identical dispersion characteristics (not shown here). It confirms

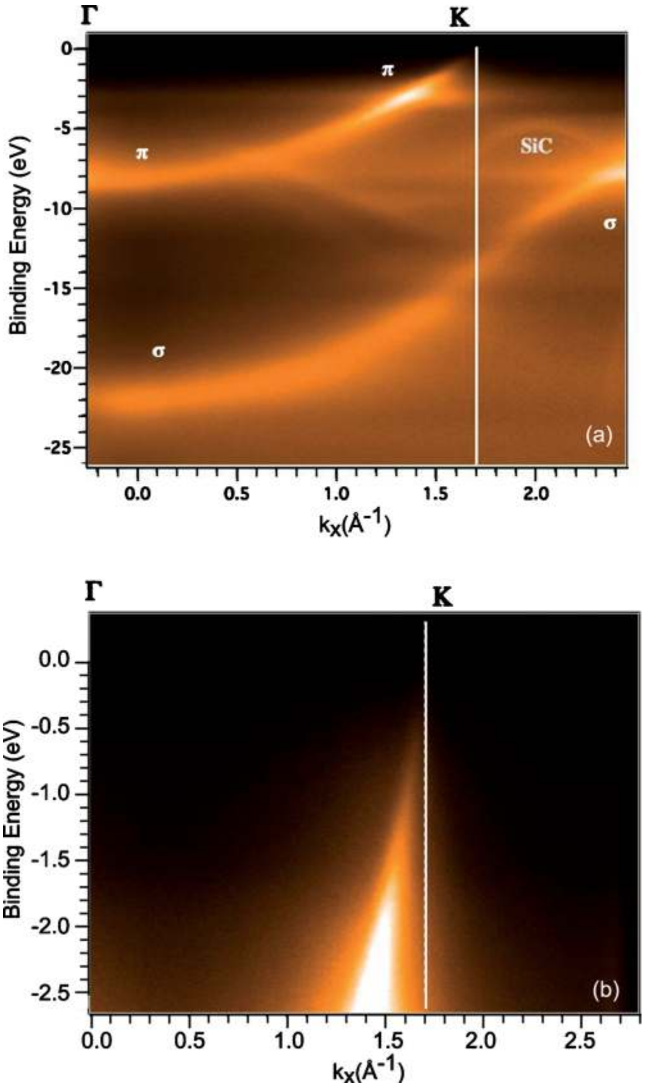

FIG. 4. (Color online) Valence band spectra ($h\nu = 110$ eV) of MBE grown graphene (25 min at 1040 °C), displaying the dispersion along ΓKM (a) and around K-point (b).

again that graphene layers behave as uncoupled graphene layers on the C-face of SiC.

A solid carbon source has been used to grow graphene on SiC $(000\bar{1})$ by molecular beam epitaxy in an UHV chamber. Topography analysis by AFM shows that such graphene layers grow without altering the initial atomically flat step and terrace structure of the substrate, contrary to the graphitization process. Photoelectron spectroscopy has been achieved to estimate the thickness of the MBE graphene and to study the valence band structure, showing the well-defined Dirac cone dispersion at the K-point. Graphene grown by MBE or obtained by graphitization basically behaves identically on the C-face of SiC, noticeably the occurrence of rotated and weakly coupled domains. The main advantage of MBE is to preserve the initial SiC surface morphology and to allow a precise control of the thickness especially at the beginning of growth (1–2 ML). These promising results encourage further study on the MBE of graphene.

This work has been achieved with the financial support of the French ANR (project Xp-Graphene) and the Nord-Pas de Calais Regional Council.

[1] I. Forbeaux, J.-M. Themlin, and J.-M. Debever, Surf. Sci. **442**, 9 (1999).

[2] J. Hass, W. A. de Heer, and E. H. Conrad, J. Phys.: Condens. Matter **20**, 323202 (2008).

[3] K. S. Novoselov, A. K. Geim, S. V. Morozov, D. Jiandg, Y. Zhang, S. V. Dubonos, I. V. Grigorieva, and A. A. Firsov, Science **306**, 666 (2004).

[4] A. Reina, X. Jia, J. Ho, D. Nezich, H. Son, V. Bulovic, M. S. Dresselhaus, and J. Kong, Nano Lett. **9**, 30 (2009).

[5] J. Wintterlin and M.-L. Bocquet, Surf. Sci. **603**, 1841 (2009).

[6] K. V. Emtsev, F. Speck, Th. Seyller, L. Ley, and J. D. Riley, Phys. Rev. B **77**, 155303 (2008).

[7] F. Varchon, P. Mallet, L. Magaud, and J.-Y. Veuillen, Phys. Rev. B **77**, 165415 (2008).

[8] F. Hiebel, P. Mallet, F. Varchon, L. Magaud, and J.-Y. Veuillen, Phys. Rev. B **78**, 153412 (2008).

[9] M. Sprinkle, J. Hicks, A. Tejeda, A. Taleb-Ibrahimi, P. Le Fèvre, F. Bertran, H. Tinkey, M. C. Clark, P. Soukiassian, D. Martinotti, J. Hass, and E. H. Conrad, J. Phys. D: Appl. Phys. **43**, 374006 (2010).

[10] E. Moreau, F. J. Ferrer, D. Vignaud, S. Godey, and X. Wallart, Phys. Status Solidi A **207**, 300 (2010).

[11] A. Al-Temimy, C. Riedl, and U. Starke, Appl. Phys. Lett. **95**, 231907 (2009).

[12] J. Hackley, D. Ali, J. DiPasquale, J. D. Demaree, and C. J. K. Richardson, Appl. Phys. Lett. **95**, 133114 (2009).

[13] F. Maeda and H. Hibino, Jpn. J. Appl. Phys. **49**, 04DH13 (2010).

[14] F. J. Ferrer, E. Moreau, D. Vignaud, S. Godey, and X. Wallart, Semicond. Sci. Technol. **24**, 125014 (2009).

[15] U. Starke and C. Riedl, J. Phys.: Condens. Matter **21**, 134016 (2009).

[16] G. G. Jernigan, B. L. VanMil, J. L. Tedesco, J. G. Tischler, E. R. Glaser, A. Davidson III, P. M. Campbell, and D. K. Gaskill, Nano Lett. **9**, 2605 (2009).

[17] K. Heinz, J. Phys.: Condens. Matter **16**, S1705 (2004).

[18] J. Hass, F. Varchon, J. E. Millan-Otoya, M. Sprinkle, N. Sharma, W. A. de Heer, C. Berger, P. N. First, L. Magaud, and E. H. Conrad, Phys. Rev. Lett. **100**, 125504 (2008).

[19] L. Magaud, F. Hiebel, F. Varchon, P. Mallet, and J.-Y. Veuillen, Phys. Status Solidi (RRL) **3**, 172 (2009).

[20] M. Sprinkle, D. Siegel, Y. Hu, J. Hicks, A. Tejeda, A. Taleb-Ibrahimi, P. Le Fevre, F. Bertran, S. Vizzini, H. Enriquez, S. Chiang, P. Soukiassian, C. Berger, W. A. de Heer, A. Lanzara, and E. H. Conrad, Phys. Rev. Lett. **103**, 226803 (2009).